Rheol Acta (2017) 56:729–742
DOI 10.1007/s00397-017-1029-9

ORIGINAL CONTRIBUTION

Theoretical correlation of linear and non-linear rheological symptoms of long-chain branching in polyethylenes irradiated by electron beam at relatively low doses

Mehdi Entezam[1] · **Mahdi Abbasi**[2] · **Mostafa Ahmadi**[3]

Received: 10 February 2017 / Revised: 10 May 2017 / Accepted: 12 July 2017 / Published online: 3 August 2017

Abstract Dynamic and transient shear and elongation flow experiments along with gel permeation chromatography (GPC) and differential scanning calorimetry (DSC) analysis are performed on linear low-density polyethylenes (LLDPEs) irradiated at doses below 25 kGy. GPC data indicate no changes in the molar mass distribution, and there are almost no changes in melt and crystallization temperatures, likewise. Contrary, dynamic shear rheological behavior including thermorheological complexity, type of reduced van Gurp-Palmen curves, and zero shear-rate viscosities all disclose growing levels of long-chain branching with irradiation dose. An inverse tube model is developed for binary blend of linear and star chains and used to extract the fraction of the branched components. Modeling results reveal progressive increase in the length and fraction of star chains, as evidenced by appearance of an anomalous double overshoot in the transient shear viscosities. Detection of strain hardening in extensional stress growth coefficient data, well-quantified by molecular stress function model, is also in agreement with the predictions of tube model.

Keywords Polyethylene · Long-chain branching · Linear rheology · Non-linear rheology · Modeling

✉ Mostafa Ahmadi
mo.ahmadi@aut.ac.ir

[1] Department of Chemical and Polymer Engineering, Faculty of Engineering, Yazd University, Yazd, Iran

[2] Institute for Technical Chemistry and Polymer Chemistry, Karlsruhe Institute of Technology, Karlsruhe, Germany

[3] Department of Polymer Engineering and Color Technology, Amirkabir University of Technology, Tehran, Iran

Introduction

Polyethylene (PE) with convenient processability, relatively good physico-mechanical properties, and low cost is a well-known commodity polymer for general applications. The wide varieties of PE grades differ in molecular structure and therefore the physical properties and processability. They are applied individually or in blends to produce objects, based on the end use and the process type. However, generally improved mechanical properties come with decrease in processability.

Rigorous efforts have continued to achieve new PE grades with desired properties as well as improved processing ability. Main methods could be classified into two categories. The first is conducted during the polymerization of PEs by the change in the operation conditions and also use of new designed catalytic systems (Liu et al. 2016a, b; Stadler et al. 2011; Ye and Zhu 2003). This method is comparatively considered costly and more sophisticated procedure. The second is executed after polymerization and prior converting the raw polymer materials to the articles. A common technique is using a proper amount of chemical crosslinking agent, such as peroxides, through the reactive extrusion (Brandolin et al. 2007; Ghosh et al. 1997; Kim and Yang 1999; Suwanda and Balks 1993). But, a practical approach for the modification of raw polymeric materials, especially polyolefins, which have frequently attracted considerable attention from both scientific and industrial points of view, is ionizing beam irradiation (Auhl et al. 2012a, b, 2004; Cheng et al. 2005, 2009; Du Plessis et al. 2006; Randall and Zoepfl 1986; Scheve et al. 1990). For this purpose, the electron and gamma irradiations are the most prevalent technologies used.

It has been well-known that irradiation can cause changes in the architecture and the molecular characteristics of the polymeric materials, depending on their structures and the

irradiation process conditions including dose, atmosphere, and temperature (Charlesby 1960; Singh and Silverman 1992). Crosslinking is the most recognized impact of irradiation on the PEs (Charlesby 1960; Qu and Rårby 1995; Singh and Silverman 1992). On this base, it has been applied to reinforce some physical and thermal properties of the PE products for a long time (Charlesby 1960; Singh and Silverman 1992). With regard to this aim, the irradiation of the products is usually performed under the ambient conditions and at a dose high enough to attain relatively great gel content (more than 60%). On the other hand, it is noteworthy that the gel formation has to be avoided in irradiation of PE as raw material, because it makes the melt processing difficult and even impossible. This could be overcome by governing the irradiation conditions, especially dose, so that commercial PE grades modified by irradiation at the relatively low dose (≤25 kGy) have been produced without any problem of flowability and even with the improved processability (Cheng et al. 2009; Du Plessis et al. 2006).

Among the changes happening during irradiation process for PE include formation of long-chain branches (LCBs) and consequent changes in the molar mass and molar mass distribution, low degree of crosslinking, and oxidation of the polymer; if irradiated in air, the two formers are considered as the most important ones to affect the properties and the flow behavior of the polymer (Cheng et al. 2005, 2009; Du Plessis et al. 2006). So, the detailed identification of these molecular structure changes due to the irradiation would be a vital bridge to predict and to describe truly the processability and the end use properties of the irradiated polymer materials.

In order to characterize LCB in the polymer chain structure, the traditional methods, like nuclear magnetic resonance (NMR), have some limitations related to interference from short-chain branches (SCB), making it difficult to distinguish short and long branches (Shroff and Mavridis 2001). On the other hand, the rheological studies have been proved to be as crucial measures with fingerprints for assessing the microstructure and the LCB characteristics of the polymer chains (García-Franco et al. 2006; Lohse et al. 2002; Read 2015; Shroff and Mavridis 1999; Stadler and Karimkhani 2011; Stadler et al. 2008; Stadler and Münstedt 2009; Takeh et al. 2011; Van Ruymbeke et al. 2005b).

There are some patents but little research works concerning the irradiation treatment of various ethylene polymers as raw material and the articles produced using them (Cheng et al. 2005, 2009; Du Plessis et al. 2006; Harbourne 1980; Kurtz and Potts 1985). To the best of our knowledge, the effect of irradiation modification on the rheological properties of ethylene polymers has not been investigated profoundly, as it has been done for the polypropylene (Auhl et al. 2012a, b, 2004). The reason might be the fact that branching can be introduced in polyethylene through free radical polymerization; however, post-polymerization modification is the only method for adding branches to the structure of polypropylene.

Linear low-density polyethylene (LLDPE) with chains of linear structure, including α-olefins as the short-chain branches, is a well-known polymer with an important application in the film production industry. Although the typical film grades of LLDPE yield usually the appropriate physical properties for the product, they show unfavorable processability in the film blowing process. This drawback comes from the lack of LCB in the chain structure of traditional Ziegler-Natta-catalyzed LLDPEs (Micic and Bhattacharya 2000). Hence, they are typically blended with low-density polyethylene (LDPE) for such an application. In this way, LCB can be introduced in the structure, to improve the processability of LLDPE film grades (Du Plessis et al. 2006; Harbourne 1980; Kurtz and Potts 1985); however, homogeneity of the final blend in the microscale and its consequences on the final mechanical properties of blend are additional problems. Improvement of melt strength without change of final mechanical properties due to the non-homogeneities is expected to be achievable by application of irradiation at relatively low doses, likewise.

In this contribution, high-energy electron beam irradiation of a film grade of LLDPE was performed at different doses lower than 25 kGy and under the ambient condition. The main objective was to study the relationship between the microstructure of LLDPE, modified by irradiation, and its rheological consequences. For this aim, the rheological properties were probed under the linear (SAOS) and non-linear deformations (transient shear and extension) and analyzed theoretically by using the TMA and MSF models, respectively. The paper is organized as follows. After description of the materials and methods for irradiation and rheological evaluations, first the linear rheological data in shear, dynamic, and transient modes will be presented. Then, the extensional deformation results will be explained, and correlations of the results with the microstructure would be represented.

Experimental

Materials

LLDPE used in this study was a commercial product (LL0209AA) from Tabriz Petrochemical Company, Iran. It contains butene-1 as comonomer. The melt flow index is 0.9 g/10 min (190 °C, 2.16 kg), and the density at room temperature is 0.91 g/cm^3.

Sample preparation

The LLDPE granules in a rectangular container with depth of 5 cm were electron-beam irradiated under the air atmosphere

at atmospheric pressure and ambient temperature with 10 Mev electrons and with different doses (d = 0, 4, 12, and 24 kGy) using an accelerator of the type Rhodotron TT200 (Ion Beam Application Company, Belgium). The irradiation geometry is schematically shown in Scheme 1. The doses were applied in a one step, and since their values are relatively low, the temperature increase resulting from the irradiation is not so high to affect the molecular structure. The average absorbed doses and the dose uniformity (the ratio of maximum adsorbed dose to minimum one within the sample palette) were measured by the cellulose triacetate (CTA) film. These values along with the sample codes are listed in Table 1.

Samples for rheological experiments were compression-molded at 170 °C into sheets with proper thicknesses using a Dr. Collin (25 MPa) laboratory hot press. It is widely known that irradiation deteriorates thermal stability; therefore, to prevent samples from thermos-oxidative degradation during the pressure molding and rheological measurements, the surfaces of the LLDPE granules were coated first with a mixture of two antioxidants (0.2% Irganox 1010 and 0.2% Irganox 245) and one stabilizer (0.2% Irgafos 38).

Methods

Molecular characterization

Molecular analyses were carried out by high-temperature size-exclusion chromatography method using the apparatus SEC-GPC (PL-220) coupled with a refractive index (RI) detector. The solvent was TCB (1,2,4-trichlorobenzene, Merck) at 150 °C.

Thermal analysis

Thermal behavior of LLDPE samples explained in Table 1 was probed by a differential scanning calorimeter (DSC-50, Ta1300, Shimadzu, Japan) under the nitrogen atmosphere.

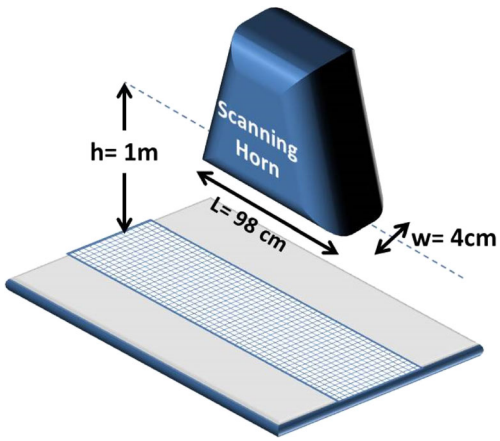

Scheme 1 The irradiation geometry

Samples were first heated from 25 °C temperature to 150 °C and held at this temperature for 3 min to eliminate the possible thermo-mechanical histories. Then, they were cooled to 25 °C and heated again to 150 °C at a heating rate of 10 °C/min. The thermal properties including the crystallization (T_c) and melting (T_m) temperatures and the degree of crystallinity were determined by cooling and second-cycle heating thermograms.

Shear rheological measurements

Linear viscoelastic shear flow experiments were performed using an Anton Paar Physica shear rheometer (MCR 300 model) equipped with parallel plate geometry (diameter = 25 mm, gap = 1 mm). The frequency sweep tests in the range of 0.05 to 500 rad/s were performed under the nitrogen atmosphere at various temperatures (T = 150, 170, 190, and 210 °C) with a strain amplitude of 5% to maintain the response of the samples in the linear viscoelastic regime. The data at different temperatures were shifted to the reference temperature of 190 °C, by horizontal shifting of the logarithmic curves of the linear viscoelastic properties versus the frequency. The activation energies (E_a) for flow of the samples were determined by considering the Arrhenius-type temperature dependence for the horizontal shift factor (a_T):

$$a_T = exp\left[\left(\frac{E_a}{R}\right)\left(\frac{1}{T}-\frac{1}{T_0}\right)\right] \quad (1)$$

where R is the gas constant and T is the absolute temperature. The subscript "0" refers to the reference temperature of 190 °C.

Uniaxial elongation rheological measurements

Extensional experiments were conducted at 210 °C using an EVF fixture and samples with rectangular shape, L = 18, W = 10, and T = 0.5 mm. Constant extensional rates from 10 to 0.003 s^{-1} were performed, so that the samples are stable enough on the drams without sagging. Samples were as much as thin (W/T ≈ 20) in order to have uniaxial stretching rather than planar extension during the experiment. A pre-stretching with rate of 10^{-3} s^{-1} was imposed on the samples before the experiments in order to compensate the minor sagging effects. Effects of pre-stretching and change of density at 210 °C compared to room temperature were included in the stress growth coefficient calculations according to literature (Aho et al. 2010). The measured transient elongation viscosity ($\eta_E^+(t,\dot{\varepsilon}_0)$) is defined in Eq. (2):

$$\eta_E^+\left(t,\dot{\varepsilon}_0\right) = \frac{\sigma(t,\dot{\varepsilon}_0)}{\dot{\varepsilon}_0} \quad (2)$$

Table 1 Definition of samples, corresponding dosimetry data, and molecular characterization and rheological properties

Sample codes	Nominal adsorbed dose (kGy)	Average absorbed dose (kGy)	Dose uniformity	M_n (kg/mol)	M_w (kg/mol)	PDI	MFI (2.16 kg)	MFI (10 kg)	MFR	G^0_N (MPa)
B1	0	0	–	33	114	3.49	0.98	5.6	5.7	1.40
B2	4	4.1	1.14	27	103	3.76	0.50	4.5	9.0	1.41
B4	12	11.4	1.19	26	103	3.99	0.08	2.1	26.3	1.49
B7	24	22.1	1.17	28	163	5.94	–	0.3	–	1.42

In order to investigate how the measured values of $\eta_E^+(t,\dot{\varepsilon}_0)$ agrees with the linear viscoelastic anticipation of this rheological parameter given as $\eta_E^+(t) = 3\eta_0^+(t)$, the transient linear shear viscosity $\eta_0^+(t)$ was calculated from the SAOS test according to:

$$\eta_0^+(t) = \int_0^t G\left(t'\right)dt' \tag{3}$$

where $G(t')$ denotes the linear shear modulus of the general linear viscoelastic Maxwell model (Graham et al. 2003):

$$\eta_0^+(t) = \int_0^t \sum_{i=1}^N g_i e^{\frac{-s}{\tau_i}} ds = \sum_{i=1}^N g_i \tau_i \left(1 - e^{\frac{-s}{\tau_i}}\right) \tag{4}$$

where g_i and τ_i are the relaxation modulus and the relaxation time of the ith element of the Maxwell model, respectively.

Results and discussion

Chain architecture as revealed by traditional characterization methods

As described before, LLDPEs are mainly used in film applications. The corresponding film blowing process requires a high-melt strength polymer to form a stable bubble. LLDPEs are therefore typically blended with branched LDPE to overcome this shortcoming. Irradiation of raw materials at relatively low doses can provide a simple alternative for introduction of required branches in the microstructure. Molar mass distributions (MMDs) of the samples are shown in Fig. 1, and the corresponding averages including the number average molar mass (Mn), the weight average molar mass (Mw), and their ratio as the polydispersity indices (PDI) are reported in Table 1. By increasing the irradiation dose up to 12 kGy, the general trend is that the low molar mass part of the distribution is slightly shifted to lower values, while the high molar mass region is almost intact, as reflected in the corresponding Mn and Mw values leading to somewhat higher PDI values. But, as realized by MMD curves, irradiation at dose of 24 kGy gives rise to more obvious changes in molecular characteristics so that a shoulder appears at high molar mass region; therefore, Mw and PDI increase significantly. Considering very low gel content (less than 1.5 wt.%) of the sample irradiated at dose of 24 kGy, the changes in MMD could be attributed to formation of LCBs in LLDPE chains. It should be mentioned that the slight changes in the molecular masses and MMD of the samples B2 and B4 could be because of nearly identical effectiveness of the two competitive phenomena, chain scission and branching, that simultaneously occur during the irradiation process. However, the branching effect, resulting in the molar mass increase, predominates at the doses high enough, as observed for sample B7 irradiated at the dose of 24 kGy. Similar results concerning irradiation of high-density polyethylene (Cheng et al. 2005) and modifications of Mw and MMD related to irradiation-induced LCB formation in polypropylene irradiated at high doses are reported (Auhl et al. 2004; Cheng et al. 2009).

Unlike the GPC data where the differences in most samples are negligible, there is a significant decrease in the melt flow index (MFI) values measured at different loads and also a considerable increase in the melt flow index ratio (MFR) for all samples. Such a decrease in MFI and increase in MFR would be generally interpreted as significant increase in molar mass and PDI values, if the polymer chains were certainly linear. However, the absence of such a difference in the corresponding MMDs of the samples irradiated at the doses of 4 and 12 kGy indicates that samples have growing levels of LCB as higher irradiation doses are utilized. Of course, MFI and MFR values of sample B7 could be affected by both LCBs formation and the increases in MW and MMD.

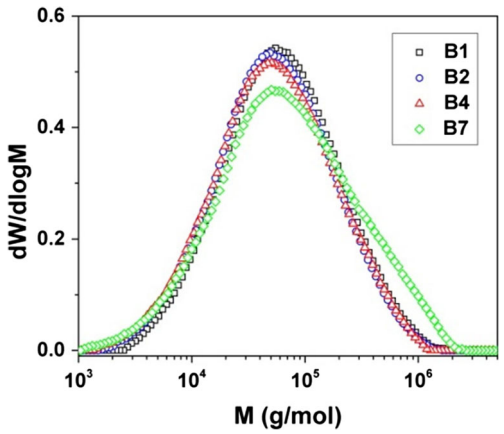

Fig. 1 Molar mass distribution of the samples

On one hand, polymer viscosity increases with LCB formation due to enhancement of the chain entanglements. This effect, in agreement with decreased MFI values, is significantly pronounced for the viscosity measured at low shear rates (Yan et al. 1999). On the other hand, due to the contraction of hydrodynamic volume of the polymer chains, the polymer is easier disentangled at higher shear rates, and therefore, it would have enhanced shear thinning rheological behavior that could be evidenced by the higher MFR values (Yan et al. 1999). On this base, LLDPE's MFR value increased by irradiation (see Table 1) could imply that irradiation facilitates processability of the samples, in contrary with the usual thought.

The utilized sample is a linear low-density PE which contains about 6 wt% of 1-butene comonomer so that the melting temperature and density are decreased from 138 °C and 0.96 g/ml of linear HDPE to 124 °C and 0.91 g/ml, as depicted in Table 2. The short-chain branching would not interfere with our investigation, as it is constant among all samples. The melting and crystallization temperatures of samples remain unchanged at different irradiation doses which implies constant lamellae thickness. In other words, it is the ethylene sequence length or the distribution fashion of 1-butene comonomers that still governs the lamellae thickness in all samples (Ahmadi et al. 2016). However, there is a meaningful increase in melting and crystallization enthalpy, which can be due to the nucleation tendency of branched chains as found for irradiated PP chains (Auhl et al. 2012a, b).

Shear rheology

Molecular and thermal characterization methods clearly indicate the presence of progressively higher amounts of LCB as the irradiation dose is increased. The traditional methods for characterization of LCB in polyolefins are solution-based chromatography or spectroscopic methods such as high-temperature GPC coupled with multi-angle laser light scattering (MALLS) or viscosity detector, or CNMR, respectively (Auhl et al. 2012a, b). However, these methods have their own limitations, including low sensitivity towards low levels of LCB, usage of toxic solvents at high temperatures, and more specifically, the spectroscopic methods cannot differentiate branches longer than six carbon atoms. By contrast, rheological measurements are very sensitive to traces of LCB, and many authors have tried to use rheology to characterize sparsely long-chain branched polymers (Auhl et al. 2012a, b; García-Franco et al. 2006; Lohse et al. 2002; Shroff and Mavridis 1999; Stadler and Karimkhani 2011; Stadler et al. 2008; Stadler and Münstedt 2009; Takeh et al. 2011; Van Ruymbeke et al. 2005b). Most of the efforts have been based on the zero shear-rate viscosity, which is not easily measurable because of very long relaxation times of branched molecules (Janzen and Colby 1999) Besides, broadening of MMD and introduction of LCB can have similar effects on the rheological properties in shear (Van Ruymbeke et al. 2005b). In this contribution instead, we would combine linear shear and nonlinear extensional measurements to provide a better insight to the changes induced in the structure of linear polymer chains due to irradiation.

Table 2 Thermal properties of the samples

Sample code	T_m (°C)	T_c (°C)	ΔH_m (J/mg)	ΔH_c (J/mg)	X_c (%)
B1	124.2	111.4	45.5	41	15.8
B2	122.1	110.9	54.7	48.2	19
B4	123.9	111.5	56.2	47.3	19.5
B7	123.2	110.7	62	54.3	21.6

Figure 2 shows the reduced van Gurp-Palmen (rdvGP) plots (phase angles versus the complex modulus ($|G^*|$) divided by the plateau modulus (G_N^0) (Trinkle and Friedrich 2001)) of frequency sweep measurements performed at four temperatures of 150, 170, 190, and 210 °C. We have avoided lower temperatures in our rheological characterizations, since the LLDPE sample is synthesized by multi-center Ziegler-Natta catalysts and should possess heterogeneous comonomer distribution (Ahmadi et al. 2016). In other words, they may contain chains with considerably low comonomer contents which crystallize at higher temperatures and contribute in elevating plateau modulus. The $|G^*|$ value at the minimum of the phase angle in normal van Gurp-Palmen (vGP) plot could be considered as the G_N^0 of the polymer (Trinkle and Friedrich 2001). However, since the minimum corresponding to the G_N^0 value does not appear in the plots of the samples, their G_N^0 value was approximated by the following equation (Liu et al. 2006):

$$G_N^0 = \frac{4}{\pi}\int_{-\infty}^{\omega_{max}} G''(\omega)\, d\ln\omega \tag{5}$$

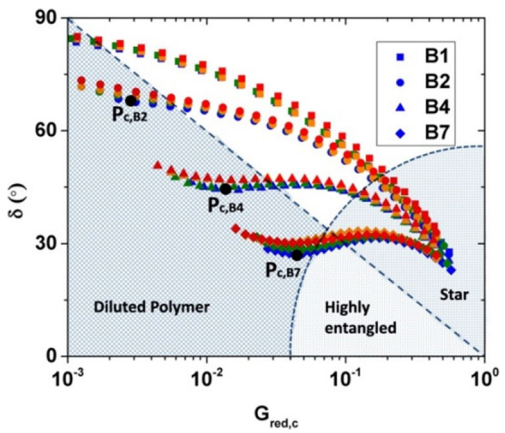

Fig. 2 The topology map of LCB polymers (Trinkle et al. 2002) and the rdvGP plots measured at 150 (*blue*), 170 (*green*), 190 (*orange*), and 210 °C (*red*) for samples B1, B2, B4, and B7

where ω_{max} stands for the frequency where loss modulus shows the maximum value. The obtained values are relatively lower than the generally accepted G_N^0 of PE (Liu et al. 2006), as expected, since the frequency that corresponds to ω_{max} is not accessible in the measured frequency and temperature domain. We have neglected this common discrepancy as the broad molar mass distribution, normally reported for Ziegler-Natta catalyzed polyolefins, and moreover, the presence of LCBs, in our case, also broaden the transition from plateau to the terminal zone and regularly avoid precise determination of plateau modulus. Nonetheless, such discrepancy does not affect our conclusion from the reduced-vGP plot, as it may cause minor shift of the curves along the abscissa. The calculated values are shown in Table 1 and used to reduce the vGP plot.

While all measurements are nicely superimposable for the B1 sample, deviation from thermorheological simplicity increases with irradiation dose. Although the highly branched low-density polyethylene (LDPE) is only slightly thermorheologically complex, for the long-chain-branched metallocene-catalyzed polyethylenes, a significant dependence of the activation energy on the relaxation time is reported (Stadler et al. 2008, 2006). At shorter relaxation times, E_a is very close to that of linear polyethylenes, but it increases at longer times. The lower E_a values are assumed to be due to linear molecules and the higher ones to long-chain-branched molecules. It has been concluded for metallocene-catalyzed polyethylenes that the thermorheological complexity is due to the presence of a mixture of linear and long-chain-branched chains, with different relaxation mechanisms and temperature dependencies (Stadler et al. 2008). Similar trend is found for linear/branched polyethylene blends (Mortazavi et al. 2016). Likewise, the thermorheological complexity reveals that the irradiation does not necessarily provide chains with similar microstructures, but chains with different topologies from linear to sparsely branched architectures, e.g., star, H-shape or combs with low number of branches could be made simultaneously. The difference between temperature dependency of the mechanism involved in relaxation of different chain architectures, i.e., reptation of linear chains, contour length fluctuation (CLF) of stars, and hierarchical relaxation of more complex architectures, results in the observed thermorheological complexity.

Independent from polymer's chemical constitute, tacticity, and composition, Trinkle et al. have drawn a topological map for LCB polymers based on the coordinates of a characteristic point $P_c(G_{red,c}, \delta_c)$ determined by local minima, as adopted and overlaid in Fig. 2 (Trinkle et al. 2002). The general trend of rdvGP plots for branched polymers is that by moving from high to low modulus, the phase angle after passing a minimum rises again and finally approaches the limiting value of 90°. The hierarchical relaxations of more complex architectures are expected to show extra local minima for each relaxation step, e.g., one minimum per each generation in dendrimers (Liu et al. 2011; Van Ruymbeke et al. 2007). Of course, the minimum is not usually observed for the crystalline linear polymers like polyethylene due to the crystallization of the polymer at temperatures necessary to reach the minimum region (Trinkle and Friedrich 2001).

The shape of rdvGP plot of the un-irradiated sample (B1) is the same as expected for the non-LCB polymers without any extra curvature. A local minima or extra curvature emerges more clearly by increasing the irradiation dose as distinguished by the corresponding Pc points in Fig. 2. These observations confirm progressive formation of LCB in LLDPE chains by increasing irradiation dose. All of the irradiated samples are located in the "Diluted polymers" section on the topology map. This means that the irradiated LLDPEs are mainly mixture of linear and randomly branched polymers (Trinkle et al. 2002), in agreement with what discussed about the thermorheological complexity of the samples.

Despite the minor thermorheological complexity, due to small activation energies which leads to shift factors near unity, best fit master-curves were made at the reference temperature of 190 °C, without any vertical shift, and the results are depicted in Fig. 3a–d. The required apparent activation energy increases from 29.9 kJ/mol for B1 to 32.9 and 37.9 for B2 and B4 samples, respectively, and decreases to 34 kJ/mol for sample B7.

The crossover point does not change upon application of small irradiation dose of 4 kGy; however, the final relaxation slopes of 1 and 2 for loss and storage moduli could not be reached, and both moduli drop with a slope between 0.5 and 1. Longitudinal Rouse relaxation and late CLF of deeper segments are mostly dominant before the crossover point, and reptation is responsible for final relaxation of linear chains, after crossover (Van Ruymbeke et al. 2005a). Therefore, the final reptation is significantly affected by the presence of sparse LCBs in sample B2. The crossover frequency decreases in sample B4, and the final relaxation slopes are further postponed, and both moduli drop with the slope of 0.5 (G', $G'' \sim \omega^{0.5}$), which is in agreement with Rouse relaxation mechanism of branched polymer segment. The crossover point totally vanishes at the highest irradiation dose for sample B7, and both moduli drop in parallel with the slope around 0.5; however, unlike the former samples, the elastic behavior is dominant in accessible frequency domain. The inset in Fig. 3d shows the master curve of an industrial LDPE with MFI = 0.85 g/10 min at 190 °C, in the same frequency domain (Tas 1994). Interestingly, the dynamic moduli clearly show terminal relaxation regime, unlike any of the irradiated samples studied here. Consequently, the microstructure of the irradiated samples is totally different from the highly branched structure expected for a free radical polymerized LDPE. Indeed, the long branches made by irradiation hinder, while the branch on branch structure of LDPE

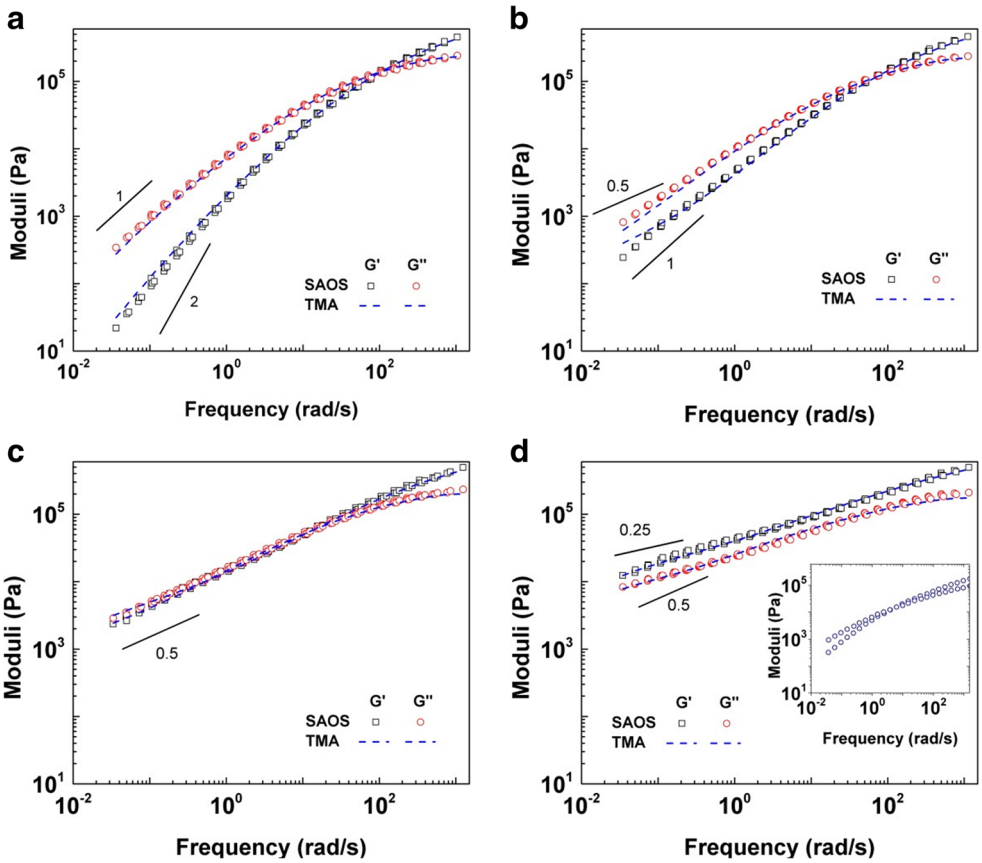

Fig. 3 Master curves of the frequency sweep measurements at 150 to 210 °C at the reference temperature of 190 °C (*symbols*) and TMA predictions (*dashed lines*) for (**a**) B1, (**b**) B2, (**c**) B4, and (**d**) B7; inset: master curve of LDPE at 190 °C

can promote terminal relaxation by contour length fluctuations.

Parallel drop of moduli has been reported for the frequency domain between two following reptation mechanisms in binary polymer blends (Struglinski and Graessley 1985). The slope of parallel drop has been used for determination of the branched chains by Robertson et al. (2004) so that "1-slope" represents the fraction of LCB chains. It could be therefore concluded that there is a progressive increase in fraction of branched chains as the irradiation dose is increased; however, no conclusion can be made about the topology of the created branched chains.

Besides the mentioned rheological characteristics, the main parameter frequently used for deduction of LCB content is zero shear-rate viscosity. Janzen and Colby have shown that there is a significant increase in viscosity if the distances between branch points are much longer than the entanglement molar mass, and there is reduction in viscosity, due to chain contraction and loss of entanglement, if the branch points are less than a few entanglements distant (Janzen and Colby 1999). Inkson et al. have derived an analytical equation to evaluate the zero shear-rate viscosity of monodisperse comb polymers, in terms of structural variables including arm length, backbone length, and the number of branches (Inkson et al. 2006). Interestingly, viscosity is exponential in arm length, consistent with specific fluctuations lifetime of branches (Ahmadi et al. 2011; Van Ruymbeke et al. 2005a), which varies with the square of backbone length and linearly with number of branches. Similarly, such a combination can lead to a significant increase in viscosity of sparsely branched chain with long arms and reduction in viscosity for heavily branched chains.

Figure 4 shows the calculated viscosity profile of the studied samples. Despite the fact that zero shear-rate viscosities cannot be reached using frequency sweep measurements and even by inclusion of start-up shear measurement data (agreement between dashed lines and symbols in the main plot of Fig. 4 confirms the applicability of Cox-Merz rule), it increases clearly with irradiation dose. The influence of the long-chain branches can be seen in a very clear fashion when picking the maximum viscosities η_{max} from the steady-state viscosity of the lowest applied shear rate in start-up shear tests and plotting them versus the weight average molar mass, as shown in the inset plot of Fig. 4. The linear reference was previously established at 150 °C (Stadler et al. 2006) and shifted to 190 °C with an activation energy E_a of 28 kJ/mol, typically found for linear HDPE (Stadler et al. 2007).

While it was not possible to determine the zero shear-rate viscosity η_0 of any of the samples within the time of stability, it is clear that η_0 is larger than the maximum viscosity measured.

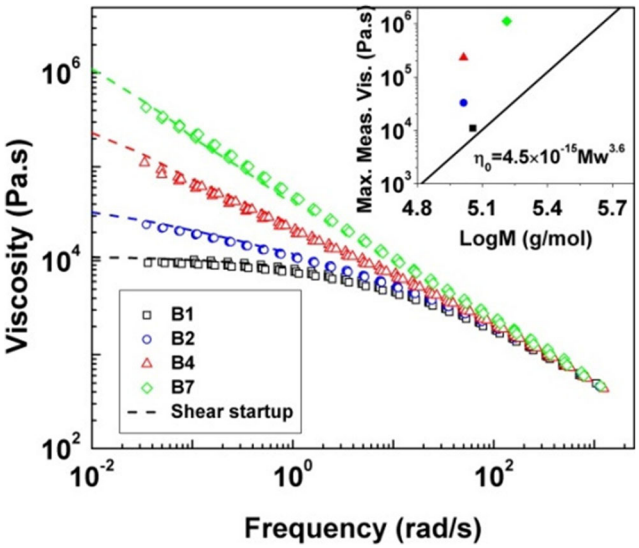

Fig. 4 Shear viscosity profiles extended by start-up shear data (main plot) and the maximum measured viscosity in start-up shear tests against the linear reference (inset plot)

Besides, despite the fact that GPC data for LCB polymers usually delivers lower molar masses, due to chain contraction, all data are located significantly above the η_0-M_w relation for linear materials (Stadler et al. 2006), which has been established as an indicator for sparsely long-chain branching but not remarkable presence of branch on branch structures (Stadler et al. 2006).

Investigation of linear rheological data on thermorheological complexity, dynamic moduli, and zero shear-rate viscosity clearly shows the presence of sparsely branched along with linear chains, whose fraction increase with irradiation dose. In order to determine the microstructure and fraction of LCB chains, a simple rheological model was developed based on time marching algorithm (TMA) (Van Ruymbeke et al. 2005a), and the samples were represented by binary blends of polydisperse linear and symmetric star chains (Ahmadi et al. 2017). Details of model development are described in Appendix A.

Theoretical curves are shown in Fig. 3 by dashed lines. The widely used tube model parameters for PE are Me = 1850 g/mol, G_N^0 =2 MPa, and $\tau_e = 2 \times 10^{-8}$ s, where Me is Graessley's entanglement molecular weight, and τ_e is Rouse relaxation time of an entanglement (Liu et al. 2006). Prior predictions based on the measured MMD values for sample B1, as shown in Fig. 3a are in very good agreement with frequency sweep data. As the number of entanglements are very high (z = Mw/Me > 60), contour length fluctuations are too slow, and reptation is the dominant relaxation mechanism.

A minor part of the MMD (with the same PDI) was considered to be turned into 3-arm star upon irradiation, whose molar mass and fraction were adjusted to capture the measured dynamic moduli, for samples B2, B4, and B7. The obtained theoretical curves are in good agreement with the measured frequency sweeps as comprehended from the error function values as defined in Eq. (a.13) and shown in Table 3. The corresponding molar mass and fraction of star chains are shown in Table 3, as well.

The molar mass of the star chains is relatively lower or equal to the mother linear chains. However, since the stars are incapable of reptation, due to the very small Me, a small fraction of stars with relatively low molar mass can impose a very long relaxation time. The fraction of stars and their length increase with the irradiation dose, as expected.

As mentioned before, irradiation produces diverse branched structures from stars to comb and even branch on branch architectures. However, in the studied irradiation doses, the frequency of more complex branched architectures is significantly lower than chains with only one long-chain branch. The proposed model is therefore a simplified representative of the real structure. Still, such a model can provide a good guess from the average structure based on the bulk rheological properties.

Linear polymer chains exhibit stress overshoots during the start-up of shear flow. The origin of this transient overshoot response is considered to be primarily chain retraction after initial stretching besides the orientation of chains and subsequent decrease in the entanglement density of the molecules (Lu et al. 2014) Recently, Snijkers et al. (2013) have shown for a comb with 29 long-chain branches that the shear stress in a start-up test displays an anomalous double overshoot. They have interpreted this behavior in view of tube-based relaxation theory. The main stress overshoot is related to the backbone

Table 3 Theoretical predictions of molar mass and fraction of star chains and comparison of irradiation dose with the obtained MSF model parameters

Sample	Linear chains		Star chains		Defined error (X)	MSF parameters		
	Mw (kg/mol)	wt.%	Mw (kg/mol)	wt.%		β_{mix}	β	f^2_{max}
B1	114	100	–	–	0.030	1	1	1
B2	114	90	98	10	0.023	1.05	1	7
B4	114	68	104	32	0.015	1.16	1.15	9
B7	114	40	117	60	0.011	1.30	1.30	>50

stretching and orientation, while the minor overshoot that happens in strains before the main overshoot is attributed to the withdrawal of long branches into the backbone tube.

Figure 5 shows the transient viscosity of samples measured at different shear rates. The double overshoot becomes apparent for sample B4 at high shear rates and more strongly for sample B7. The double overshoot in transient viscosity could be either due to presence of long-chain branching, as suggested by Snijkers et al. (2013), but more probably can be an indication of the presence of two different structures (linear and sparsely branched chains) with significantly different responses to non-linear shear measurements. In this way, start-up shear data can also confirm the presence of branched chains; however, quantitative judgment still needs further investigations.

Extensional rheology

Figure 6 represents the results of the extensional experiments in the framework of stress growth coefficient data along with Doi-Edwards (DE) and MSF predictions. Details of the developed MSF model are described in Appendix b. Linear viscoelastic, LVE, curves (dashed lines) were plotted using relaxation spectra by fitting the Maxwell model on the SAOS data in the range of experimental frequency window. However, due to the lack of SAOS data of B4 and B7 at low-frequency range, G' and G'' have not reached slopes 2 and 1, respectively. Therefore, whole relaxation spectra, especially longest relaxation times, were not achieved for B4 and B7. In order to have better fitting of MSF model on the stress growth coefficient data at low extensional rates and long times (longer than the inverse of minimum frequency in SAOS data), we added additional longer relaxation spectra by fitting the Maxwell elements, g_i, τ_i, on the lower extensional rates than the inverse of minimum achieved frequency in SAOS data, i.e., 0.05 rad/s. Following procedure was used to fit the MSF model on the experimental data:

- Fitting the Maxwell model on G' and G'' data by adjusting the 5–6 elements, g_i and τ_i, to cover the frequency range of 500–0.05 rad/s.
- Fitting the parameter β of MSF model to achieve the best fit for the onset of strain hardening for extensional rates in the range from 10 to 0.1 s^{-1}.
- Fitting the parameter f_{max} of MSF model to achieve the best fit for the maximum of stress growth coefficients at extensional rates larger than 0.1 s^{-1}; however, this maximum (steady-state extensional viscosity) has not reached in some of the extensional rates for B4 and all of rates for B7; therefore, f_{max} was adjusted in order to have the best fit on the present data.

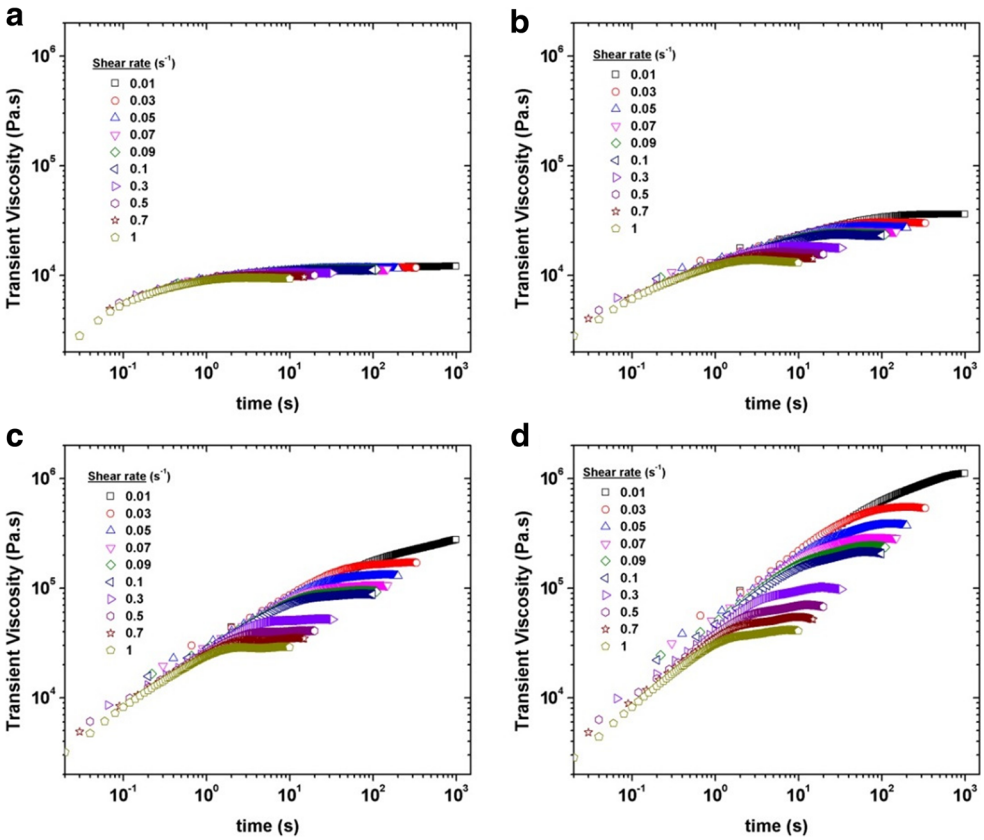

Fig. 5 Transient shear viscosity at various shear rates for (**a**) B1, (**b**) B2, (**c**) B4, and (**d**) B7

– Fitting the additional 1–4 elements of Maxwell model with longer relaxation times on the data at extensional rates lower than 0.1 s^{-1}.

Figure 6 shows that DE model, considering a constant tube diameter at different strains, is unable to account for any strain hardening in extensional flows, while MSF constitutive equation could fairly predict this phenomenon in stress growth coefficient data for all of the samples. The increase in the irradiation dose increases the strain hardening of the samples.

Sample B1 does not show any strain hardening, and steady-state value of extensional viscosity (plateau region) is below the LVE curve. MSF theory predicts the $\beta = 1$ and $f_{max} = 1$, In these structures the proves the linear topology in B1. While B2, B4, and B7 clearly show the strain hardening behavior demonstrating the presence of LCB structures in them. The intensity (slope) of onset of strain hardening predicted by $\beta > 1$ shows that B2, B4, and B7 has a sparsely branched structure, e.g., star-like. With respect to the definition of parameter β for branched polymers ($\beta = M/M_{bb}$, the ratio of total molecular weight to that of backbone), a symmetric star topology has $\beta = 1.5$; however, for asymmetric star topologies and considering the two longest arms as backbone span and shortest arm as single-side chain, a theoretical value of $\beta < 1.5$ is calculated. A higher value of β was fitted on the extensional data for commercial LDPE (Abbasi et al. 2012; Rolón-Garrido et al. 2009; Wagner et al. 2003) and radiated long-chain branched polypropylene (Bahreini et al. 2017; Wagner et al. 2006), which prove the presence of combs and cayley tree structures, which volume (weight) fraction of branches in a molecule is higher than their backbone. According to the previous assumption that radiated samples contained binary blends of linear and symmetric star chains and also the calculated weight fractions of star and linear parts (Table 3), a linear mixing rule (Abbasi et al. 2012) might be used to predict the parameter β for such a sparsely branched system:

$$\beta_{mix} = \sum_{i=1}^{N} \varphi_i \beta_i \tag{6}$$

where φ_i is the weight fraction of linear ($\beta = 1$) or symmetric star ($\beta = 1.5$) parts. Table 3 shows the β_{mix} values for all of samples predicted from the weight fractions of linear viscoelastic model (TMA model), which are very close to the predicted β values from fitting the non-linear viscoelastic model (MSF model) on the stress growth coefficient data in Fig. 6.

Values of β above 1.5 and 2 are typical of highly branched comb and treelike topographies like tubular and autoclave LDPEs, respectively (Abbasi et al. 2012, 2013). Maximum stress growth coefficient at all extensional rates is observable at Hencky strain around 3; however, this region is reached only at low extensional rates for B4. While B7 breaks before reaching steady-state extensional viscosity; therefore, a constant value governed by f_{max} in MSF model cannot be predicted accurately; however, a

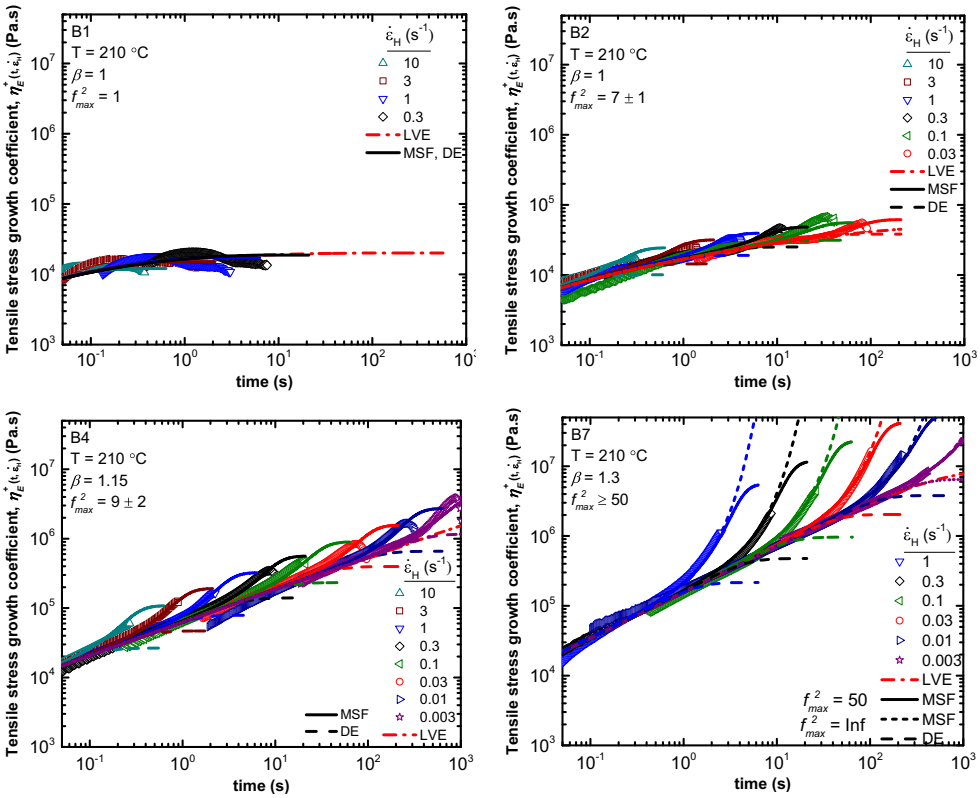

Fig. 6 Tensile stress growth coefficient data at 210 °C along with MSF constitutive equation predictions with two constant parameters β and f_{max} for samples B1, B2, B4, and B7

minimum value f^2max ≈ 50 is probable. Figure 7 shows both predictions by f^2_{max} = 50 and infinitive value for B7 by solid and broken lines, respectively. Maximum stretching of polymer chains, f_{max}, could be related to both length and number (or branch-point distance) of branches; however, in such star molecules (or sparsely branched structures), only length of arms determines the maximum stretching of molecule. Therefore, the lengths of arms in Table 3, defined by TMA model, are in agreement with the f_{max} fitted on the non-linear extensional data.

Strain hardening is amplified in case when a backbone segment is trapped between two branching points like comb- or tree-like structures. However, the origin of strain hardening basically refers to increasing of strain rate above the inverse of stretching time of a chain, τ_s. This stretching time is equal to the Rouse time of a linear chain, $\tau_{Rouse} = \tau_e Z^2$. This means that at enough high extensional rates or low temperature or in case of an enough high molecular weight, a linear polymer could show strain hardening. For example, a linear PS with Mw = 390 kg/mol and Rouse time τ_{Rouse} = 329 s at 130 °C show strain hardening at $\dot{\varepsilon} > 0.01\ s^{-1}$ (Bach et al. 2003). This stretching time is higher than the Rouse time of a branched polymer (e.g., for Comb topology $\tau_{Rouse} = Z_{bb}(Z_{bb} + N_{br}Z_{br})\tau_e$, bb standing for the backbone and br for the branch) because this Rouse time definition only includes the friction effects of side chains but not the length (entanglements) of side chains (see Lentzakis et al. 2013). In other words, a side arm in a star molecule could increase the stretching time due to its friction effect (even if it is not entangled) and due to the entanglements with neighbor molecules.

Strain hardening is reported to be very sensitive to chain architecture. The so-called strain hardening factor (SHF) is defined as the ratio between the maximum of tensile stress growth coefficient divided by the three times of transient shear viscosity (Trouton's ratio). As is clear from Fig. 7, strain hardening factor decreases by increasing strain rate in B2 and B4 samples, while for sample B7, it increases initially and decreases at higher extension rates. Reduction of strain hardening with increasing strain rate is frequently attributed to the presence of sparsely branched chains, while the opposite behavior is typical of highly branched chains with a topology-like LDPE (Auhl et al. 2012b). Evidently, irradiation at relatively low doses predominantly creates PEs with sparsely branched chains, and branched on branched structure can only be made using high irradiation intensities.

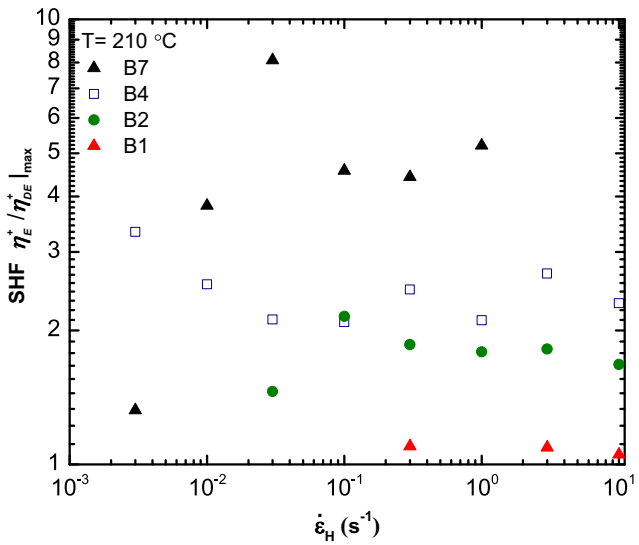

Fig. 7 Strain hardening factor as a function of strain rate for the studied samples

Conclusions

Irradiation at relatively low doses can improve processability of LLDPEs as raw materials while keeping the crystalline phase and corresponding properties almost intact. In this work, a commercial Ziegler-Natta-catalyzed LLDPE is irradiated by electron beam at three relatively low doses (<25 kGy). While the MMD data could barely show any changes and thermal properties are almost intact, qualitative rheological properties like MFI and MFR show significant changes. The reduced van Gurp-Palmen plots revealed the presence of branched chains as local minima, whose intensity increases with irradiation dose. The corresponding dynamic moduli also revealed that while the mother linear sample shows terminal relaxation slopes in the accessible frequency zone, the irradiated samples show parallel drop of moduli with progressively lower slopes. The increased zero shear-rate viscosities confirmed the branching is sparse and heavily branched chains are negligible. A tube-based model was therefore developed to represent the structures by binary blends of polydisperse linear and star chains. The theoretical curves could nicely capture the measured moduli by adjusting the molar mass and fraction of star component. The obtained results clearly confirmed increasing fraction of stars with longer arms as the irradiation dose was elevated. The start-up shear experiments also showed anomalous double overshoots that was attributed to coexistence of stars with significantly different response to non-linear shear, compared to the linear chains. Finally, extensional measurements also revealed higher strain hardening for irradiated samples. The MSF model was used to interpret the obtained data. The parameters of MSF model (β and f_{max}) were in agreement with the predictions of TMA model and confirmed presence of sparsely (star-like)-branched chains, likewise.

Tube-based model for linear rheology

A tube-based model was developed to predict the linear rheological behavior of irradiated samples. It was assumed that irradiation at low doses as used here can lead to formation of symmetric star chains and fraction of more complicated structures is negligible.

Symmetric stars can mainly relax by contour length fluctuations according to the following probability:

$$p_{fluc}(x,t) = \exp\left(\frac{-t}{\tau_{fluc}(x)}\right) \quad \text{(a.1)}$$

The specific lifetime for fluctuations is determined by free Rouse motions for the segments near extremities, while deeper segments need to overcome the potential penalty to retract:

$$\tau_{early}(x) = \frac{9\pi^3}{16}\tau_e \times^4 Z^4 \quad \text{(a.2)}$$

$$\tau_{late}(x) = \tau_0 \exp\left(\frac{U(x)}{kT}\right) \quad \text{(a.3)}$$

$$U(x) = \frac{3kT}{2Nb^2}\left(L_{eq}x\right)^2 + cons \quad \text{(a.4)}$$

Since the relaxation times of deep segments are exponentially separated in time space, they can use the already relaxed part of the chain as solvent to dilate the confining tube according to dynamic dilution. Transition between the early and late fluctuations modes happens at the segment where the potential barrier is equal to the system's thermal energy.

Besides contour length fluctuations, the linear chains can also reptate at the specific reptation lifetime:

$$p_{rept}(x,t) = \sum_{i,\text{odd}} \frac{4}{i\pi}\sin\left(\frac{i\pi x}{2}\right)\exp\left(\frac{-i^2 t}{\tau_{rept}}\right) \quad \text{(a.5)}$$

$$\tau_{rept} = 3\tau_e Z^3 \phi^{\alpha}_{active}(t) \quad \text{(a.6)}$$

where $\varphi_{\text{active}}(t)$ is the fraction of already relaxed segments that reptation can use to dilate the confining tube based on the Graessley's criterion and $\alpha = 1$ is the dilution exponent (Van Ruymbeke et al. 2005a).

The fraction of oriented chains can be calculated at each time, from the fraction of segments that are relaxed neither by reptation nor by fluctuations:

$$\phi(t) = \sum_i \varphi_i \int_0^1 \left(p_{rept}(x,t)p_{fluc}(x,t)\right)dx \quad \text{(a.7)}$$

where ϕ_i is the weight fraction of chain i. As the other chains present in the system can also relax, the confining tube also relaxes by constraint release process. The probability of tube relaxation is equal to the probability of chain relaxation, while it cannot be faster than what lateral Rouse movements may allow:

$$\phi_{CR}(t_i) \geq \phi_{CR}(t_{i-1})\left(\frac{t_{i-1}}{t_i}\right)^{0.5} \quad \text{(a.8)}$$

The transient modulus can be calculated by inclusion of high frequency fast modes and longitudinal slow modes of Rouse motion:

$$G(t)\Big/G_N^0 = \phi(t)\phi^{\alpha}_{CR}(t) + F_{Rouse,long}(t) + F_{Rouse,fast}(t) \quad \text{(a.9)}$$

$$F_{Rouse,long}(t) = \sum_i \frac{\varphi_i}{4Z_i}\sum_{j=1}^{Z_{i-1}} \exp\left(\frac{-j^2 t}{\tau_{Rouse,i}}\right) \quad \text{(a.10)}$$

$$F_{Rouse,fast}(t) = \sum_i \frac{5\varphi_i}{4Z_i}\sum_{j=Z_i}^{N} \exp\left(\frac{-2j^2 t}{\tau_{Rouse,i}}\right) \quad \text{(a.11)}$$

where Z corresponds to the chain's span, and the specific Rouse relaxation time is:

$$\tau_{Rouse} = \tau_e Z^2 \quad \text{(a.12)}$$

The molar mass distributions of both linear and star chains were considered to follow log-normal distribution function with similar PDI (Table 2). The mother linear chain had a constant molar mass as shown in Table 3, while the molar mass and fraction of star chains were adjusted using Nelder-Mead simplex method to capture the dynamic moduli measured by frequency sweep. The following error function was defined, and the obtained values are shown in Table 3:

$$\chi = \frac{1}{n}\sum_{i=1}^{n}\left[\frac{\left(G'_{exp}(i) - G'_{the}(i)\right)^2}{G'_{exp}(i)^2} + \frac{\left(G''_{exp}(i) - G''_{the}(i)\right)^2}{G''_{exp}(i)^2}\right] \quad \text{(a.13)}$$

Molecular stress function model

Extensional data were analyzed using molecular stress function (MSF) constitutive equation which is a molecular model based on Doi-Edwards and reptation concept with taking to account the backbone stretching. This model can predict and quantify the strain hardening in extensional flows using two non-linear parameters, β and $f_{\max}$ (Rolón-Garrido 2014). Constant β represents the ratio of entanglements in polymer, $Z = Z_b + N_{br} \times Z_a$, to its backbone, Z_b, and governs the slope of strain hardening. Parameter $f_{\max}$ is related to the maximum stretching of the backbone and determines the steady-state value of the stress growth coefficient, $\eta^{+}_{E,\max}$ in extensional flows. Here, we used a version of MSF model which was presented by Abbasi et al. (2012) and verified using different branched polymers in different non-linear deformations (Abbasi et al. 2013):

$$\boldsymbol{\sigma}(t) = \Sigma_{i=1}^{N} \int_{-\infty}^{t} \frac{g_i}{\tau_i} e^{\frac{(t-t')}{\tau_i}} f^2\left(t,t'\right) \mathbf{S}_{DE}^{IA}\left(t,t'\right) dt' \tag{b.1}$$

$$\mathbf{S}_{DE}^{IA} = 5\mathbf{S} = 5\left[\left(\frac{1}{J-1}\right)\mathbf{B} - \left(\frac{1}{(J-1)\left(I_2 + 13/4\right)^{0.5}}\right)\mathbf{C}\right] \tag{b.2}$$

$$J = I_1 + 2\left(I_2 + 13/4\right)^{0.5} \tag{b.3}$$

$$\frac{\partial f}{\partial \varepsilon} = \frac{1}{2}\beta f\left(S_{11} - S_{22} - \frac{f^2-1}{f_{\max}^2-1}\sqrt{S_{11} + 0.5S_{22}}\right) \tag{b.4}$$

where bolded elements **σ**, **S**, **B**, and **C** are stress, measure of strain, Finger, and Cauchy tensors, respectively. I_1 and I_2 are the trace (invariants) of **B** and **C**, respectively. Relaxation spectra g_i and τ_i are obtained by fitting Maxwell model on linear viscoelastic data G′ and G″. Stretching function, f, shows the stretch of backbone, which causes the strain hardening phenomenon in the polymer chains and is a function of Hencky strain, ε, and non-linear parameters, β and $f_{\max}$. Equations b.1–b.4 represent an integral time-strain separable constitutive equation, which will be fitted on the uniaxial stress growth coefficient data by adjusting the β and $f_{\max}$ as fitting parameters. These parameters were used as a bridge between the strain hardening criteria and branching content.

References

Abbasi M, Ebrahimi NG, Nadali M, Esfahani MK (2012) Elongational viscosity of LDPE with various structures: employing a new evolution equation in MSF theory. Rheol Acta 51:163–177

Abbasi M, Ebrahimi NG, Wilhelm M (2013) Investigation of the rheological behavior of industrial tubular and autoclave LDPEs under SAOS, LAOS, transient shear, and elongational flows compared with predictions from the MSF theory. J Rheol 57:1693–1714

Ahmadi M, Bailly C, Keunings R, Nekoomanesh M, Arabi H, Van Ruymbeke E (2011) Time marching algorithm for predicting the linear rheology of monodisperse comb polymer melts. Macromolecules 44:647–659

Ahmadi M, Mortazavi SMM, Ahmadjo S, Zahmati M, Valieghbal K, Jafarifar D, Rashedi R (2016) Evaluation of continuous and discrete melting endotherms in determination of structural heterogeneities in Ziegler-Natta catalyzed linear low density polyethylene. Polyolefins J 3:135–146

Ahmadi M, Pioge S, Fustin C-A, Gohy J-F, van Ruymbeke E (2017) Closer insight in the structure of moderate to densely branched combs by combining modeling and linear rheological measurements. Soft Matter 13:1063–1073

Aho J, Rolón-Garrido VH, Syrjälä S, Wagner MH (2010) Measurement technique and data analysis of extensional viscosity for polymer melts by Sentmanat extensional rheometer (SER). Rheol Acta 49:359–370

Auhl D, Stange J, Münstedt H, Krause B, Voigt D, Lederer A, Lappan U, Lunkwitz K (2004) Long-chain branched polypropylenes by electron beam irradiation and their rheological properties. Macromolecules 37:9465–9472

Auhl D, Stadler FJ, Münstedt H (2012a) Rheological properties of electron beam-irradiated polypropylenes with different molar masses. Rheol Acta 51:979–989

Auhl D, Stadler FJ, Münstedt H (2012b) Comparison of molecular structure and rheological properties of electron-beam-and gamma-irradiated polypropylene. Macromolecules 45:2057–2065

Bach A, Almdal K, Rasmussen HK, Hassager O (2003) Elongational viscosity of narrow molar mass distribution polystyrene. Macromolecules 36:5174–5179

Bahreini E, Aghamiri SF, Wilhelm M, Abbasi M (2017) Influence of molecular structure on the foamability of polypropylene: linear and extensional rheological fingerprint. J Cell Plast. doi:10.1177/0021955X17700097

Brandolin A, Sarmoria C, Failla MD, Vallés EM (2007) Mathematical modeling of the reactive modification of high-density polyethylene. Effect of vinyl content. Ind Eng Chem Res 46:7561–7570

Charlesby A (1960) Atomic radiation and polymers: international series of monographs on radiation effects in materials. Elsevier

Cheng S, Dehaye F, Bailly C, Biebuyck J-J, Legras R, Parks L (2005) Studies on polyethylene pellets modified by low dose radiation prior to part formation. Nucl Instrum Methods Phys Res, Sect B 236:130–136

Cheng S, Phillips E, Parks L (2009) Improving processability of polyethylenes by radiation-induced long chain branching. Radiat Phys Chem 78:563–566

Du Plessis TA, Cheng S, Seute H (2006) Radiation treated ethylene polymers and articles made from said polymers. Google Patents

García-Franco CA, Harrington BA, Lohse DJ (2006) Effect of short-chain branching on the rheology of polyolefins. Macromolecules 39:2710–2717

Ghosh P, Dev D, Chakrabarti A (1997) Reactive melt processing of polyethylene: effect of peroxide action on polymer structure, melt rheology and relaxation behaviour. Polymer 38:6175–6180

Graham RS, Likhtman AE, McLeish TC, Milner ST (2003) Microscopic theory of linear, entangled polymer chains under rapid deformation including chain stretch and convective constraint release. J Rheol 47:1171–1200

Harbourne DA (1980) Manufacture of film from partially crosslinked polyethylene. Google Patents

Inkson N, Graham R, McLeish T, Groves D, Fernyhough C (2006) Viscoelasticity of monodisperse comb polymer melts. Macromolecules 39:4217–4227

Janzen J, Colby R (1999) Diagnosing long-chain branching in polyethylenes. J Mol Struct 485:569–584

Kim YC, Yang KS (1999) Effect of peroxide modification on melt fracture of linear low density polyethylene during extrusion. Polym J 31:579–584

Kurtz SJ, Potts JE (1985) Low level irradiated linear low density ethylene/alpha-olefin copolymers and film extruded therefrom. Google Patents

Lentzakis H, Vlassopoulos D, Read D, Lee H, Chang T, Driva P, Hadjichristidis N (2013) Uniaxial extensional rheology of well-characterized comb polymers. J Rheol 57:605–625

Liu C, He J, Van Ruymbeke E, Keunings R, Bailly C (2006) Evaluation of different methods for the determination of the plateau modulus and the entanglement molecular weight. Polymer 47:4461–4479

Liu J, Yu W, Zhou C (2011) Polymer chain topological map as determined by linear viscoelasticity. J Rheol 55:545–570

Liu P, Liu W, Wang WJ, Li BG, Zhu S (2016a) A comprehensive review on controlled synthesis of long-chain branched polyolefins: part 1, single catalyst systems. Macromol React Eng 10:156–179

Liu P, Liu W, Wang WJ, Li BG, Zhu S (2016b) A comprehensive review on controlled synthesis of long-chain branched polyolefins: part 2, multiple catalyst systems and prepolymer modification. Macromol React Eng 10:180–200

Lohse D, Milner S, Fetters L, Xenidou M, Hadjichristidis N, Mendelson R, Garcia-Franco C, Lyon M (2002) Well-defined, model long chain branched polyethylene. 2. Melt rheological behavior. Macromolecules 35:3066–3075

Lu Y, An L, Wang S-Q, Wang Z-G (2014) Origin of stress overshoot during startup shear of entangled polymer melts. ACS Macro Lett 3:569–573

Micic P, Bhattacharya SN (2000) Rheology of LLDPE, LDPE and LLDPE/LDPE blends and its relevance to the film blowing process. Polym Int 49:1580–1589

Mortazavi SMM, Jafarian H, Ahmadi M, Ahmadjo S (2016) Characteristics of linear/branched polyethylene reactor blends synthesized by metallocene/late transitional metal hybrid catalysts. J Therm Anal Calorim 123:1469–1478

Qu B, Rårby B (1995) Radiation crosslinking of polyethylene with electron beam at different temperatures. Polym Eng Sci 35:1161–1166

Randall JC, Zoepfl FJ (1986) Polymer and irradiation treatment method. Google Patents

Read DJ (2015) From reactor to rheology in industrial polymers. J Polym Sci B Polym Phys 53:123–141

Robertson CG, García-Franco CA, Srinivas S (2004) Extent of branching from linear viscoelasticity of long-chain-branched polymers. J Polym Sci B Polym Phys 42:1671–1684

Rolón-Garrido VH (2014) The molecular stress function (MSF) model in rheology. Rheol Acta 53:663–700

Rolón-Garrido VH, Pivokonsky R, Filip P, Zatloukal M, Wagner MH (2009) Modelling elongational and shear rheology of two LDPE melts. Rheol Acta 48:691–697

Scheve BJ, Mayfield JW, DeNicola Jr AJ (1990) High melt strength, propylene polymer, process for making it, and use thereof. Google Patents

Shroff R, Mavridis H (1999) Long-chain-branching index for essentially linear polyethylenes. Macromolecules 32:8454–8464

Shroff R, Mavridis H (2001) Assessment of NMR and rheology for the characterization of LCB in essentially linear polyethylenes. Macromolecules 34:7362–7367

Singh A, Silverman J (1992) Radiation processing of polymers

Snijkers F, Vlassopoulos D, Ianniruberto G, Marrucci G, Lee H, Yang J, Chang T (2013) Double stress overshoot in start-up of simple shear flow of entangled comb polymers. ACS Macro Lett 2:601–604

Stadler FJ, Karimkhani V (2011) Correlations between the characteristic rheological quantities and molecular structure of long-chain branched metallocene catalyzed polyethylenes. Macromolecules 44:5401–5413

Stadler FJ, Münstedt H (2009) Correlations between the shape of viscosity functions and the molecular structure of long-chain branched polyethylenes. Macromol Mater Eng 294:25–34

Stadler FJ, Piel C, Klimke K, Kaschta J, Parkinson M, Wilhelm M, Kaminsky W, Münstedt H (2006) Influence of type and content of various comonomers on long-chain branching of ethene/α-olefin copolymers. Macromolecules 39:1474–1482

Stadler FJ, Gabriel C, Münstedt H (2007) Influence of short-chain branching of polyethylenes on the temperature dependence of rheological properties in shear. Macromol Chem Phys 208:2449–2454

Stadler FJ, Kaschta J, Münstedt H (2008) Thermorheological behavior of various long-chain branched polyethylenes. Macromolecules 41:1328–1333

Stadler FJ, Arikan-Conley BA, Kaschta J, Kaminsky W, Münstedt H (2011) Synthesis and characterization of novel ethylene-graft-ethylene/propylene copolymers. Macromolecules 44:5053–5063

Struglinski MJ, Graessley WW (1985) Effects of polydispersity on the linear viscoelastic properties of entangled polymers. 1. Experimental observations for binary mixtures of linear polybutadiene. Macromolecules 18:2630–2643

Suwanda D, Balks S (1993) The reactive modification of polyethylene. I: The effect of low initiator concentrations on molecular properties. Polym Eng Sci 33:1585–1591

Takeh A, Worch J, Shanbhag S (2011) Analytical rheology of metallocene-catalyzed polyethylenes. Macromolecules 44:3656–3665

Tas PP (1994) Film blowing: from polymer to product

Trinkle S, Friedrich C (2001) Van Gurp-Palmen-plot: a way to characterize polydispersity of linear polymers. Rheol Acta 40:322–328

Trinkle S, Walter P, Friedrich C (2002) Van Gurp-Palmen plot II—classification of long chain branched polymers by their topology. Rheol Acta 41:103–113

Van Ruymbeke E, Keunings R, Bailly C (2005a) Prediction of linear viscoelastic properties for polydisperse mixtures of entangled star and linear polymers: modified tube-based model and comparison with experimental results. J Non-Newtonian Fluid Mech 128:7–22

Van Ruymbeke E, Stéphenne V, Daoust D, Godard P, Keunings R, Bailly C (2005b) A sensitive method to detect very low levels of long chain branching from the molar mass distribution and linear viscoelastic response. J Rheol 49:1503–1520

Van Ruymbeke E, Orfanou K, Kapnistos M, Iatrou H, Pitsikalis M, Hadjichristidis N, Lohse D, Vlassopoulos D (2007) Entangled dendritic polymers and beyond: rheology of symmetric Cayley-tree polymers and macromolecular self-assemblies. Macromolecules 40:5941–5952

Wagner M, Yamaguchi M, Takahashi M (2003) Quantitative assessment of strain hardening of low-density polyethylene melts by the molecular stress function model. J Rheol 47:779–793

Wagner MH, Kheirandish S, Stange J, Münstedt H (2006) Modeling elongational viscosity of blends of linear and long-chain branched polypropylenes. Rheol Acta 46:211–221

Yan D, Wang W-J, Zhu S (1999) Effect of long chain branching on rheological properties of metallocene polyethylene. Polymer 40:1737–1744

Ye Z, Zhu S (2003) Synthesis of branched polypropylene with isotactic backbone and atactic side chains by binary iron and zirconium single-site catalysts. J Polym Sci A Polym Chem 41:1152–1159